DEEJ (2020) 9 (5) 25-40

University of Kashan

Desert Ecosystem Engineering Journal

Journal homepage: http://deej.kashanu.ac.ir

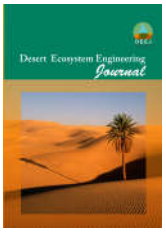

Simulating the Effect of Climate Change on Soil Erosion Risk in Two Regions, Tal Siah and Anar Sheitan Forest (Kerman Province, Iran)

Saeid Barkhori[1], Arezoo Sharifi[2*], Hossein Asadi[3], Maryam Nasabpour Molaei[4], Jaber Salehpoor[5]

Received: 19/04/2020 Accepted: 29/12/2020

Abstract

Soil erosion is an important environmental problem worldwide. Climate change can affect soil erosion by changing the rainfall pattern; hence, it is essential to assess climate change and its effect on soil erosion in different regions. This study aimed to predict the effect of climate change on soil erosion risk using the RUSLE model in Anar Sheitan forest and Tal Siah area in Jiroft region. For this purpose, meteorological station data, remote sensing images, and GIS techniques were used to prepare the necessary model inputs. Three climate change scenarios, RCP2.6, RCP4.5 and RCP8.5, were simulated in three 2006-2025, 2046-2065, and 2080-2099 periods. The rainfall erosivity factor was estimated for these periods in order to assess the impact of climate change on soil erosion risk using existing meteorological data. Other factors of the RUSLE model were considered constant, and soil erosion risk was calculated for each scenario in each period using the ArcGIS software. The analysis of results under RCP8.5 scenario during 2006-2025 period and RCP8.5 scenario during 2080-2099 period indicated that the average soil erosion risk dropped from 0.8 to 1.2 ton ha^{-1} $year^{-1}$ in Anar Sheitan forest, reflecting an surge of 0.4 ton $ha^{-1}year^{-1}$. Furthermore, soil erosion risk spiked from 0.23 to 0.35 ton ha^{-1} $year^{-1}$ in Tal Siah, suggesting a surge of 0.1 ton $ha^{-1}year^{-1}$. Overall, the results suggest that the soil loss will be higher in the future, which may be partly prevented by watershed management and soil conservation practices.

Keywords: Statistical downscaling model (SDSM), soil conservation, remote sensing, climate change scenario, Sentinel-2.

1. Assistant Professor, Department of Ecological Engineering, Faculty of Natural Resources, University of Jiroft, Kerman, Iran
2. Ph.D. Student in Soil Physics and Conservation, Department of Soil Science and Engineering, Vali-e-Asr University of Rafsanjan, Iran; Arezoo_sha62@yahoo.com
3. Associate Professor, Soil Science Department, College of Agriculture and Natural Resources, University of Tehran, Karaj, Iran
4. Forests, Range and Watershed Management Organization, Jiroft, Kerman, Iran
5. M.Sc. Graduated in Water Resources Engineering, Department of Water Engineering, Faculty of Agricultural Sciences, University of Guilan, Rasht, Iran
DOI: 10.22052/jdee.2020.227498.1064

1. Introduction

Sediment load transport to rivers is a critical issue in the conservation of water resources, which is directly influenced by the soil erosion. Accelerated erosion and human-induced erosion can cause damage not only in farms and range lands, but also in the area subjected to erosion. Reduced productivity and the degradation of soil physical and chemical properties are among onsite effects of erosion. Offsite damages include the deposition of sediments on fertile agricultural lands and pastures, the filling of water supply sources and irrigation channels, and the pollution of water bodies by sediments, heavy metals, and chemicals (Hengl, 2006). Global climate change affects rainfall pattern, which can ultimately affect rainfall intensity, surface runoff, soil erosion, and even vegetation (Azimi Sardari et al. 2019).

Since field monitoring of soil erosion is both time consuming and costly, various models have been developed to estimate soil erosion. These models consist of conceptual (Schuol et al., 2008), physical (Nord & Esteves, 2005) and empirical models (Ferreira et al., 2015). The Revised Universal Soil Loss Equation (RUSLE) is an empirical model extensively used in recent years (Honarmand et al, 2011; Panagopoulos et al., 2015; Ferreira et al., 2015; Gaubi et al., 2017; Asadi et al., 2017; Patowary & Sarma, 2018; Mohammadi et al., 2018). The RUSLE model allows to evaluate the climate change impact on soil erosion risk (Nearing et al., 2004; Yang et al., 2015). This model is capable of predicting the rainfall erosivity factor (R) using climate change scenarios (Hoomehr et al, 2016).

Several studies on the impact of climate change on soil erosion risk have integrated the remote sensing technique, GIS and RUSLE equation (Prasannakumar et al., 2012; Asadi et al., 2018). In the United States, Segura et al. (2014) examined the impact of climate change on the soil erosion. They first studied changes in rainfall erosivity in nine different climates using three general circulation models under three scenarios, B1, A2 and A1B. Azimi Sardari (2019) modeled the impact of land use and climate change scenarios on soil erosion using the RUSLE model in Minab drainage basin. In another study, RCP2.6, RCP4.5 and RCP8.5 scenarios were employed to simulate the R factor, and CA-Markov model was utilized to simulate the land use factor.

Jiroft region in southeastern Iran is of great importance not only for the agricultural products, but also for its natural resources (i.e. forest and range lands). For example, the *Tecomella undulata* (Anar Sheitan) forest, a rare and invaluable tree species, is abundant in this region. Therefore, this study aimed to evaluate the impact of climate change on soil erosion risk under three scenarios of RCP2.6, RCP4.5, and RCP8.5 in three periods of 2006-2025, 2046-2065, and 2080-2099. The RUSLE model was used to estimate the soil erosion risk, which was considered as a variable in the model. The risk of soil erosion was assessed at different periods to adopt the necessary management for soil conservation in the future according to the erosion status.

2. Materials and methods

2.1. Study Area

Two separate areas, Anar Sheitan forest and Tal Siah area, in the vicinity of Jiroft were selected to explore the effect of climate change on the soil erosion risk (Figures 1 and 2).

Anar Sheitan, dominated with *Tecomella undulata,* is the largest protected forest reserve and one of the notable habitats of this shrub. It is located 25 kilometers to the north of Jiroft, covering an area of 40 hectares. *Tecomella Undulata*, a rare species of the *Bignoniaceae* family, is particularly important for a raft of reasons such as desertification, pharmaceutical usage, wood industry and soil erosion conservation. With a warm and semi-temperate climate, this region has an average

annual rainfall of 180 mm coupled with winter precipitation. It has scorching summers and mild winters, with its minimum temperature rarely falling below zero. Soil is relatively deep and gravelly with a sandy loam texture (Amiri, 2019).

Tal Siah is 5 km away from Jiroft city with an area of about 2539 hectares. According to Jiroft weather station, which is the closest station to the study area, the average rainfall in this region is 173 mm per year, with a maximum and minimum temperature of 49 and -4 degrees, respectively. Dominant with Aridisols, the area is host to diverse plant species includeing *Ziziphus*, *Cabulica, Prosopis*, *Calligonum comosum*, *Problica aphylla*, and *Cuminum cyminum*. Since 2015, the Natural Resources Organization of Jiroft has planted several species including *Acacia*, *Ziziphus*, and *Prosopis* cineraria in the region at 10 m intervals (Roodab Paydar Consulting Engineers, 2011).

2.2. Soil Sampling and Sample Preparation

For accurate sampling, the sampling points were identified on 1: 25000 topographic maps and land use maps and their latitudes and longitudes were recorded. By selecting 25 points for each land use of Anar Sheitan forest and Tal Siah region, a total of 50 points were identified. Using GPS, the points selected on map were marked on the ground (Figure 1). To determine soil properties, samples were taken from 0 to 10 cm depths. They were then transferred to the laboratory and dried before determining the soil texture by the hydrometric method (Gee and Bauder, 1982). The soil organic carbon was measured by the wet oxidation method (Walkley and Black, 1934).

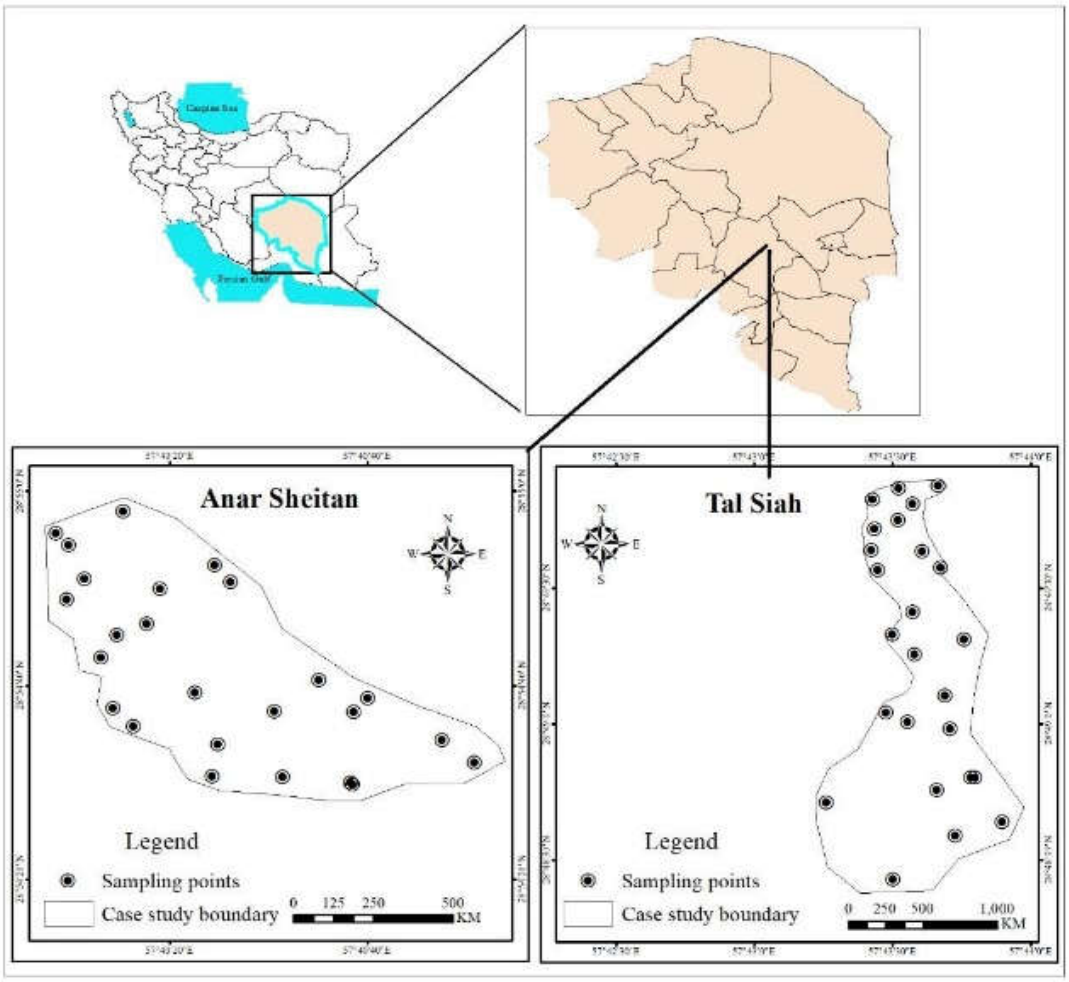

Figure (1): The sampling points for Anar Sheitan and Tal Siah

2.3. Data collection

The research data included 30layers of -m digital elevation model (DEM), rainfall data obtained from meteorological stations (7 stations, Figure 3, Table 1), and the Sentinel-2 satellite images taken on July 18, 2018 to produce vegetation maps. To this end, the images were corrected in terms of atmospheric correction by the Sen2cor in SNA. They were used in later stages after applying necessary preprocessing.

2.4. Climate Change Simulation

In the present study, observational data were obtained from 7 stations within and around the study area in a baseline statistical period (1990 to 2005). They were then controlled and evaluated in terms of data quality. The metrological-stations included Dalfard, Dehroud, Dowlatabad, Fathabad, Kahnouj, Sabzevaran. SDSM 5.1 model was used for rainfall data downscaling and the evaluation of climate change impact on stations in future according to baseline data (Wilby and Harris, 2006). Accordingly, precipitation and temperature can be simulated from 2006 to 2100 using a baseline period (Wilby and Harris, 2006). In order to simulate future rainfall, rainfall data were examined in three periods (2006-2025, 2046-2065, and 2080-2099) under three scenarios of RCP2.6 (optimistic), RCP4.5 (intermediate), and RCP8.5 (pessimistic) (Van Vuuren et al., 2011). Finally, the accuracy of SDSM simulation was evaluated using RMSE, NSE and R2 indices (Hassan et al., 2014).

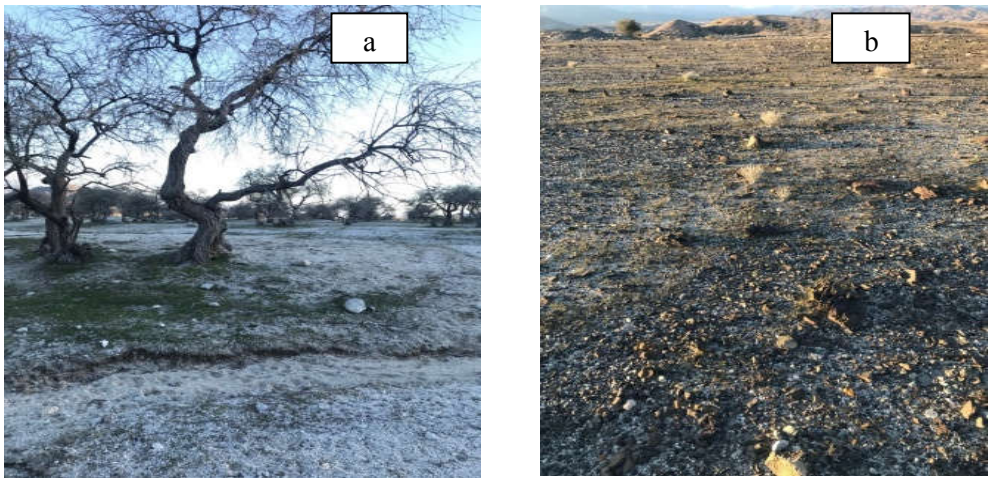

Figure (2): a. Anar Sheitan forest; b. desert and rock varnish of Tal Siah (Winter 2019)

2.5. Soil Erosion Modeling

In this study, The Revised Universal Soil Loss Equation (RUSLE) model was used to estimate soil erosion risk. The RUSLE is able to predict soil loss, which serves as a guideline for soil conservative planning (Renard et al, 1991). In this water erosion estimation model, there are factors that affect erosion (Wischmeier & Smith, 1978).

$$A = R \times K \times L \times S \times C \times P \quad (1)$$

A: the average annual soil erosion (t ha^{-1} y^{-1}); R: rainfall and runoff erosivity factor (MJ mm ha^{-1} y^{-1} h^{-1}); K: soil erodibility factor (t h MJ^{-1} mm^{-1}); L and S (LS): slope length and steepness factor; C: cover and management factor; and P: support and conservation practices factor. LS, C and P: dimensionless.

2.5.1. Rainfall erosivity (R)

The effect of climate change on soil erosion was investigated through its effect on the rainfall erosivity in the present research. Fournier Rainfall Erosivity index is widely used for the prediction and mapping of rainfall erosivity, especially for regions that lack

rainfall intensity data (Fathizad et al, 2014; Asadi et al, 2017; Bedoui, 2019). Therefore, first eligible stations were selected in the statistical period, and then the shared base time was determined followed by quality control. The simulated precipitation data derived from SDSM over 2006-2100 period was obtained for 7 rain-gauge stations within and around the basin. In the next step, the Fournier index, as an indicator of erosivity, was obtained from all stations according to Equation 2 (Renard & Freimund, 1994).

$$F = \frac{\sum_{i=1}^{12} P_i^2}{P} \quad (2)$$

where, P_i is the average rainfall in month I and P is the average annual rainfall (both in millimeters). Given the strong correlation of index with R factor, it was used to obtain the erosivity factor (Asadi et al., 2018). Interpolation methods were also used to map this factor. In the present study, since the RMSE of the IDW method is lower than other methods, it was used to calculate the erosivity factor in each period. Table 1 and Figure 3 show the positions and altitude of the stations used to calculate erosivity.

Table (1): Information about Stations used for erosivity factor

Number	Station name	Longitude	Latitude	Altitude (m)
1	Dalfard	57.63	28.97	1755
2	Dehroud	57.75	28.86	1060
3	Dowlatabad	57.14	28.72	1734
4	Fathabad	57.15	28.66	1755
5	Kahnuj	57.74	28.02	520
6	Sabzevaran	57.73	28.67	684
7	Safarzadeh	57.59	28.78	927

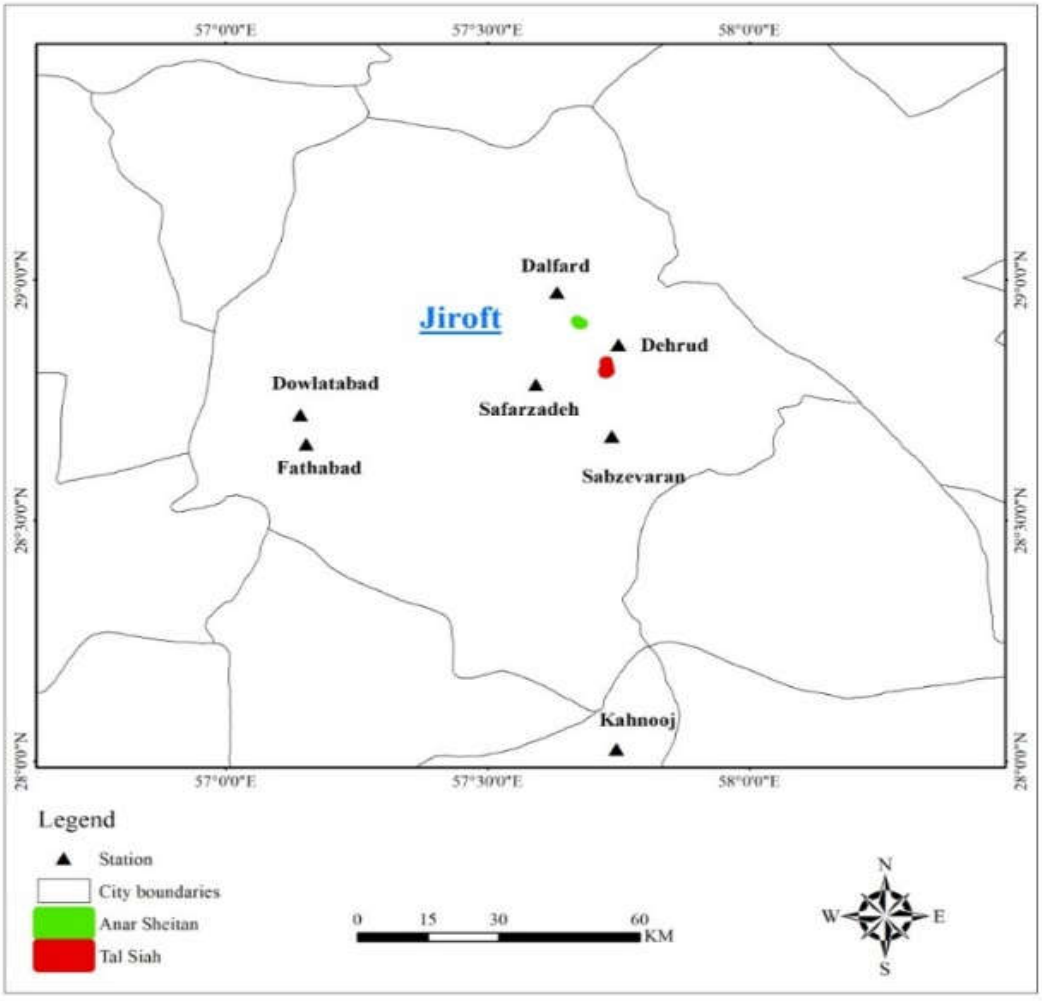

Figure (3): Location of seven meteorological stations in Jiroft and Kahnuj

2.5.2. Soil erodibility (K)

It is measured by the modified formula (Wischmeier & Smith, 1978) proposed by Renard et al. (1997). To this end, the percentages of sand, silt, clay, and organic matter content were first measured by laboratory tests, and then the soil structure and soil permeability class were determined. Equation 3 was also used to estimate the K factor (Teng et al, 2016). In this equation, M is the soil texture (the percentage of silt and fine sand); OM is the organic matter percentage; s is soil structure class, and p is permeability class. Finally, the points were converted into a layer after determining the erodibility of each point using the IDW interpolation method.

$$K = \left[\frac{2.1 \times 10^{-4} \times M^{1.14} \times (12 - OM) + 3.25 \times (s - 2) + 2.5 \times (p - 3)}{100}\right] \times 0.1317 \quad (3)$$

2.5.3. Topography (LS)

This factor indicates the effect of slope length and steepness on the amount, speed and potential of runoff erosivity (Moore & Wilson, 1992, Moore & Burch, 1986).

$$LS = \left[\frac{A_S}{22.13}\right]^{0.4} \times \left[\frac{\sin b}{0.0896}\right]^{1.3} \quad (4)$$

Where, A_s is the cumulative upstream flow of basin, and b is the area slope in radians. The necessary data layers were developed to create a topography factor map using the 30-me DEM and the topographic map was extracted from the equation above.

2.5.4. Cover and management cover (C)

C factor indicates the amount of soil loss in the cultivated land versus bare soil obtained from the same piece of land under continuous fallowing in the absence of plant residuals or cover (Wischmeier & Smith, 1978). In the present study, Sentinel-2 satellite data were used to compute this factor. Moreover, C factor was estimated using satellite images according to the formula proposed by Lin et al. (2002) because this method provided a more accurate estimation of the C-factor in arid and semiarid regions (Anache et al, 2014). Hence, NDVI was first calculated according to Eq. 5, and then the vegetation cover (C) was predicted from the layer according to Eq. 6.

$$\mathrm{NDVI} = (\mathrm{NIR} - \mathrm{RED})/(\mathrm{NIR} + \mathrm{RED}) \quad (5)$$

$$\mathrm{C} = (-\mathrm{NDVI} + 1)/2 \quad (6)$$

2.5.5. Support and conservation practices factor (P)

In general, conservation measures describe cultivation on contour lines, strip cultivation, and terracing. The P-factor value equals 1 when there is no conservation measure in the region. In this study, this factor was considered to be 1 in both regions.

This study sought to predict the effects of climate change on soil erosion risk in Anar Sheitan forest and Tal Siah region using the RUSLE model under climate change scenarios. In the first step, the climate change data were simulated for three periods (2006-2025, 2046-2065, and 2080-2099) using the SDSM (Azimi Sardari et al, 2019). Three validity indices, R2, RMSE and Nash-Sutcliffe efficiency (NSE), were used to assess the validity of simulation results. Then, the rainfall erosivity factor was estimated from simulated data under different scenarios and periods as a dynamic factor. Other factors of the RUSLE model, including soil erodibility, topography, vegetation cover, and soil conservation, as constants in the model, were measured by ground sampling, remote sensing technique, and GIS. The layers were integrated into the RUSLE model using ArcGIS software, and soil erosion was investigated in different periods and scenarios. Figure 4 shows the general flowchart of the research process.

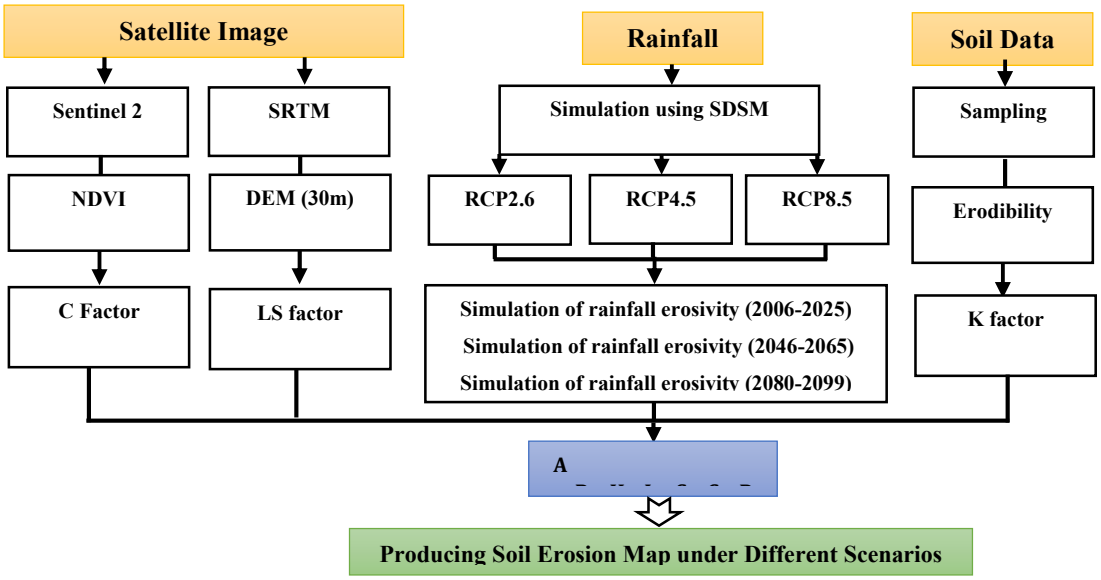

Figure (4): Flowchart of the process steps

3. Results and discussion

3.1. Climate change and regional erosivity

Table 2 lists the results of accuracy evaluation of SDSM in the precipitation downscaling using R^2, RMSE, and Nash-Sutcliffe efficiency (NSE) indices for seven climatologically stations. The results indicate a strong relationship between the simulated and observed data. High values of R^2 and NS and low values of RMSE suggest that the SDSM could be used to model climate changes in the future.

After confirming the validity of the climatic modeling of precipitation, the rainfall erosivity was calculated from Eq. 2 for seven stations during 2006-2099 period. The results of three scenarios in these three periods are presented in Table 3 & 4. As shown in Table 3, the highest erosivity was related to 2080-2099 period and RCP8.5 scenario. Also, as depicted in Table 4, Dalfard station had the highest erosivity among all sites and periods. In addition, the lowest erosivity was reported in Fathabad and Dowlatabad stations under RCP8.5 scenario.5, and Sabzevaran station under RCP2.6 scenario.

Table (2): Accuracy assessment of the SDSM using observational data at the stations

Station name	RMSE	NSE	R^2
Dalfard	7.7	0.94	0.98
Dehroud	8.38	0.91	0.97
Dowlatabad	4.21	0.87	0.95
Fathabad	1.93	0.97	0.98
Kahnouj	5.5	0.86	0.97
Sabzevaran	2.88	0.95	0.99
Safarzadeh	6.6	0.82	0.91

Table (3): Mean and standard deviation of erosivity data under different scenarios for Anar Sheitan and Tal Siah

Scenario		R2.6			R4.5			R8.5	
Name	SD / Mean	2005-2026	2046-2065	2080-2099	2005-2026	2046-2065	2080-2099	2005-2026	2046-2065	2080-2099
Anar	SD	0.46	0.39	0.49	0.42	0.54	0.39	0.48	0.44	0.51
Sheitan	Mean	50.13	46.68	51.56	50.85	58.83	53.36	53.76	55.46	63.48
Tal Siah	SD	0.87	0.69	0.90	0.78	0.95	0.70	0.88	0.78	0.89
	Mean	34.9	34.4	35.45	37.10	41.34	40.6	38.01	41.07	47.12

Different scenarios over three periods (2006-2025, 2046-2065, and 2080-2099) in Anar Sheitan forest and Tal Siah region are shown in Figures 5 & 6. The study of spatial

variability of erosivity in Anar Sheitan forest indicated that erosivity in the northern parts of the region was greater than the southern regions in all periods. On the other hand, erosivity changes ranged from 45 to 65 (MJ mm ha^{-1} $y^{-1}h^{-1}$) in different periods.

Many studies have estimated the degree of erosivity at district, provincial, and national levels for Iran (Nikkami and Mahdian, 2015).

Table (4): Erosivity index (MJ mm ha^{-1} y^{-1} h^{-1}) for the stations in different climatic periods

Scenario	R2.6			R4.5			R8.5		
Station name	2005-2026	2046-2065	2080-2099	2005-2026	2046-2065	2080-2099	2005-2026	2046-2065	2080-2099
Dalfard	58	53	60	58	68	60	62	63	72
Dehroud	39	47	51	46	44	48	51	47	47
Dowlatabad	26	23	29	24	27	23	20	23	21
Fathabad	25	21	20	20	21	22	25	20	21
Kahnouj	37	35	25	35	29	37	31	31	43
Sabzevaran	18	21	18	22	23	27	21	26	30
Safarzadeh	30	27	26	36	29	32	28	34	35

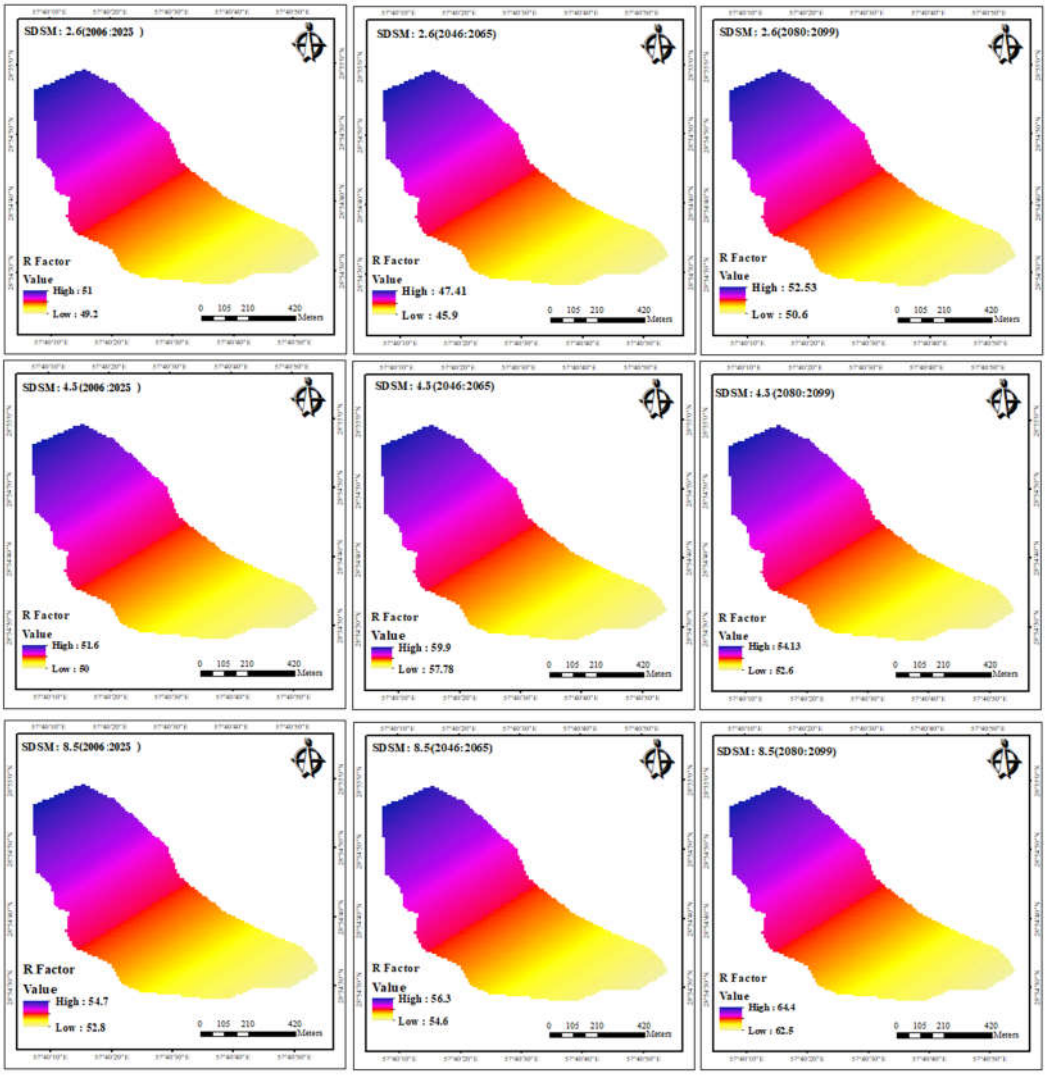

Figure (5): Changes in erosivity under scenarios of RCP2.6 (optimistic), RCP4.5 (intermediate) and RCP8.5 (pessimistic) for three periods in Anar Sheitan forest

Azimi Sardari et al. (2019) investigated the effect of climate change on soil erosion in Hormozgan. The estimated erosivity in Minab, Hormozgan province, was 30 to 35 (MJ mm ha^{-1} $y^{-1}h^{-1}$) during climatic periods, which is close to the estimated value in the present study. Furthermore, Sadeghi and Hezbavi (2015) estimated the least erosivity value (20 MJ mm ha^{-1} $y^{-1}h^{-1}$) in Bam station. In the study of Nikkami & Mahdian (2015), this value was 25 (MJ mm ha^{-1} $y^{-1}h^{-1}$). Given the location of Bam station in Kerman province and its proximity to the study area, the results of this study can be compared to those reported by Sadeghi and Hezbavi (2015) and Nikkami & Mahdian (2015). In the same vein, Panagos et al. (2017) observed that the average erosivity in this province was below 100 (MJ mm ha^{-1} $y^{-1}h^{-1}$), which is consistent with the findings of the present study. It is worth mentioning that the present study is different from other studies in terms of the degree of erosivity, which could be attributed to different stations, erosivity estimation methods, and time intervals of investigating the factor.

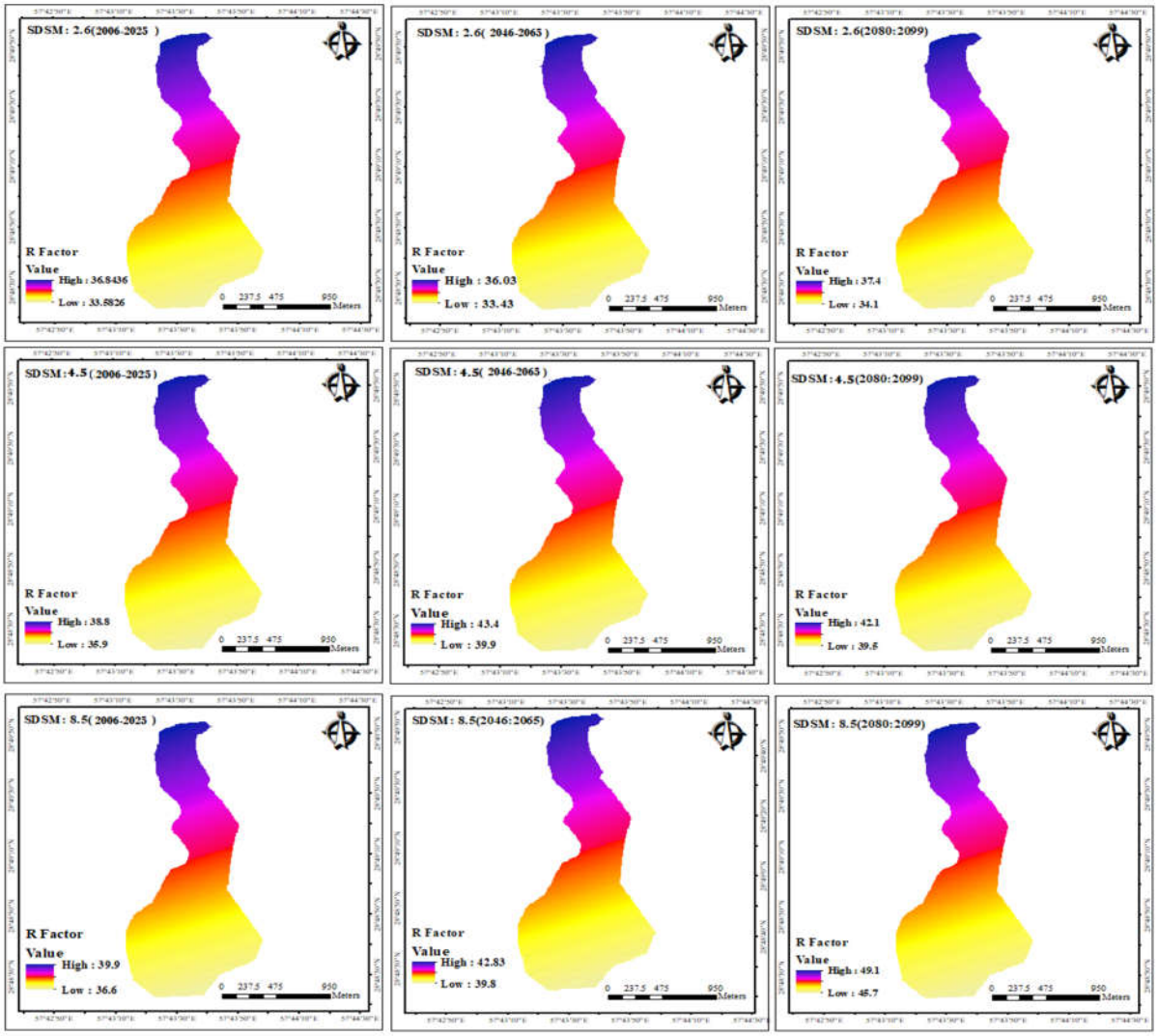

Figure (6): Changes in erosivity under scenarios of RCP2.6 (optimistic), RCP4.5 (intermediate) and RCP8.5 (pessimistic) for three periods in Tal Siah region

3.2. Soil erodibility, vegetation status, and regional topography

Figures 7 show the maps of LS, C, and K factors. as constants of the RUSLE model, in both regions. A shown in Figure 7a, the soil erodibility factor ranged from 0.08 to 0.018 (t

h MJ^{-1} mm^{-1}) in Anar Sheitan forest; however, the soil in southern part was more susceptible to soil erosion. The topographic factor in the study region ranged from 0.01 in flat areas to 40 in sloping areas. Also, the vegetation cover varied from 0.42 to 0.5. As depicted in Figure 7, the vegetation cover in the middle parts of Anar Sheitan forest is greater than other parts. In addition, the analysis of soil erodibility factor in Tal Siah indicated that soil erodibility in the southern and middle areas surpassed other parts K factor variations were in the range of 0.01 to 0.04 (t h MJ^{-1} mm^{-1}). The topographic factor value was in the range of 0.01 to 14 for Tal Siah region. Therefore, it had lower slope than Anar Sheitan forest in terms of slope and its length. Furthermore, the vegetation factor varied from 0.46 to 0.49, with its maximum value being observed in the southern region and the minimum in the middle area due to the dense vegetation. It is worth noting that the vegetation cover was extremely low in both regions and the soil was devoid of a proper vegetation cover. When there is no vegetation in the soil and the value of factor is 1, the risk of soil loss will be fairly high. On the contrary, when the vegetation is rich and the value of this factor approaches zero, the vegetation protects soil from erosion.

3.3. Soil erosion risk map

The soil erosion risk map of the two regions over different time periods is shown in Figures 8 and 9. These maps are prepared by integrating information layers obtained from the RUSLE model. According to the results, the highest soil erosion risk (the annual soil loss) in both Anar Sheitan forest and Tal Siah regions was related to 2080-2099 period under RCP8.5 scenario and its rainfall erosivity was also extremely high (Table 3). These values ranged from 13.1 to 6.3 ton ha^{-1} $year^{-1}$, particularly on a small scale in both regions, mainly in steep and uncovered areas.

Comparison of soil erosion risk in two regions suggested that the risk of soil erosion is higher in Anar Sheitan forest than in Tal Siah due to its topography and elevated slope. Figure 7 shows a greater topographic factor due to the high slope of Anar Sheitan forest. Despite the fact that Anar Sheitan forest is a protected area and the rain cannot directly impact the soil surface due to the canopy of trees; however, since the cover is sparse, the vegetation is unable to overcome the erosive power of rain and land slope. Therefore, the soil erosion was greater than Tal Siah (Figures 8 and 9). Field studies conducted by the authors in this area reveal that soil erosion in Anar Sheitan forest is greater than Tal Siah region (Sharifi et al, 2020). According to the results, Tal Siah region had less organic matters and high clay content. Therefore, since these particles can move easily, they are expected to be exceedingly eroded. However, the greater erosion in the Anar Sheitan forest than in Tal Siah suggests that the effect of topography and erosivity exceeds the inherent properties of soil in the regions. On the other hand, the desert or rock varnish, which covers the entire surface of Tal Siah region, is protected against the direct impact of raindrops (Figure 2). Since raindrops are the leading cause of interrill erosion, the least interrill erosion was observed in the region. Given the above cases, the results of this study are consistent with those on the soil erosion of regions (Figure 2).

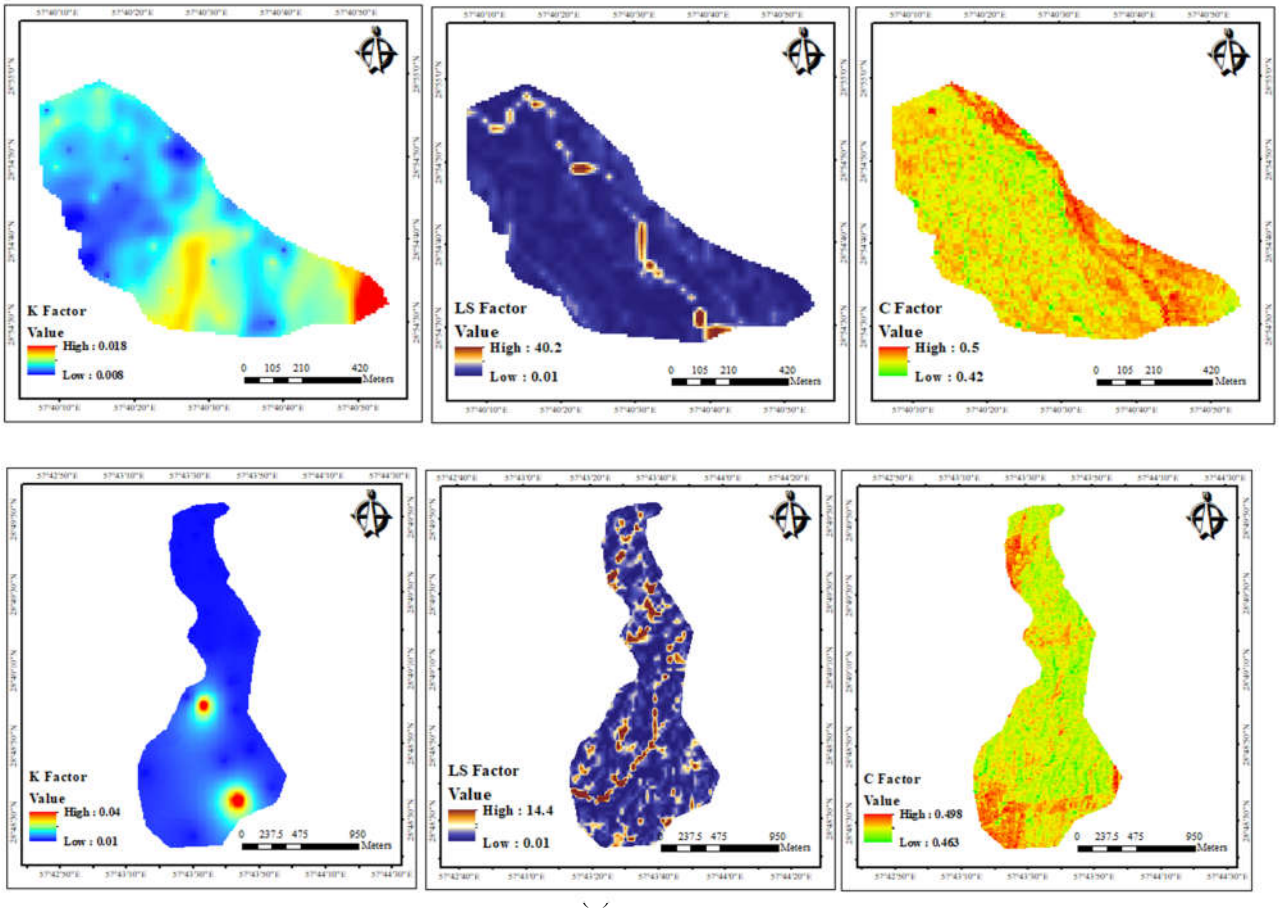

Figure (7): Map of C, LS, and K factors for a) Anar Sheitan forest, and b) Tal Siah

According to the results of Anar Sheitan forest, the average soil erosion risk spiked from 0.8 under the RCP8.5 scenario in 2006-2025 period to 1.2 ton ha^{-1} $year^{-1}$ under the RCP8.5 scenario in 2080-2099 period, indicating an growth of 0.4 ton ha^{-1} $year^{-1}$ (50% increase) in the region. In Tal Siah region, the value increased from 0.23 to 0.35 in the same period, indicating an surge of 0.12 ton ha^{-1} $year^{-1}$ (52% increases). In addition, the soils in these regions are not only susceptible to water erosion, but also prone to wind erosion because these regions have dry, loose and sensitive soil, and deprived of suitable vegetation to control wind erosion. Therefore, in the absence of rainfall in these regions, wind erosion will prevail due to the dryness of surface soils. This type of erosion will waste a large volume of soil in the region (Mohammadi et al, 2011; Kardavani, 2005). Therefore, regional management can play a significant role in reducing soil loss by maintaining and enhancing the vegetation through biological and mechanical methods.

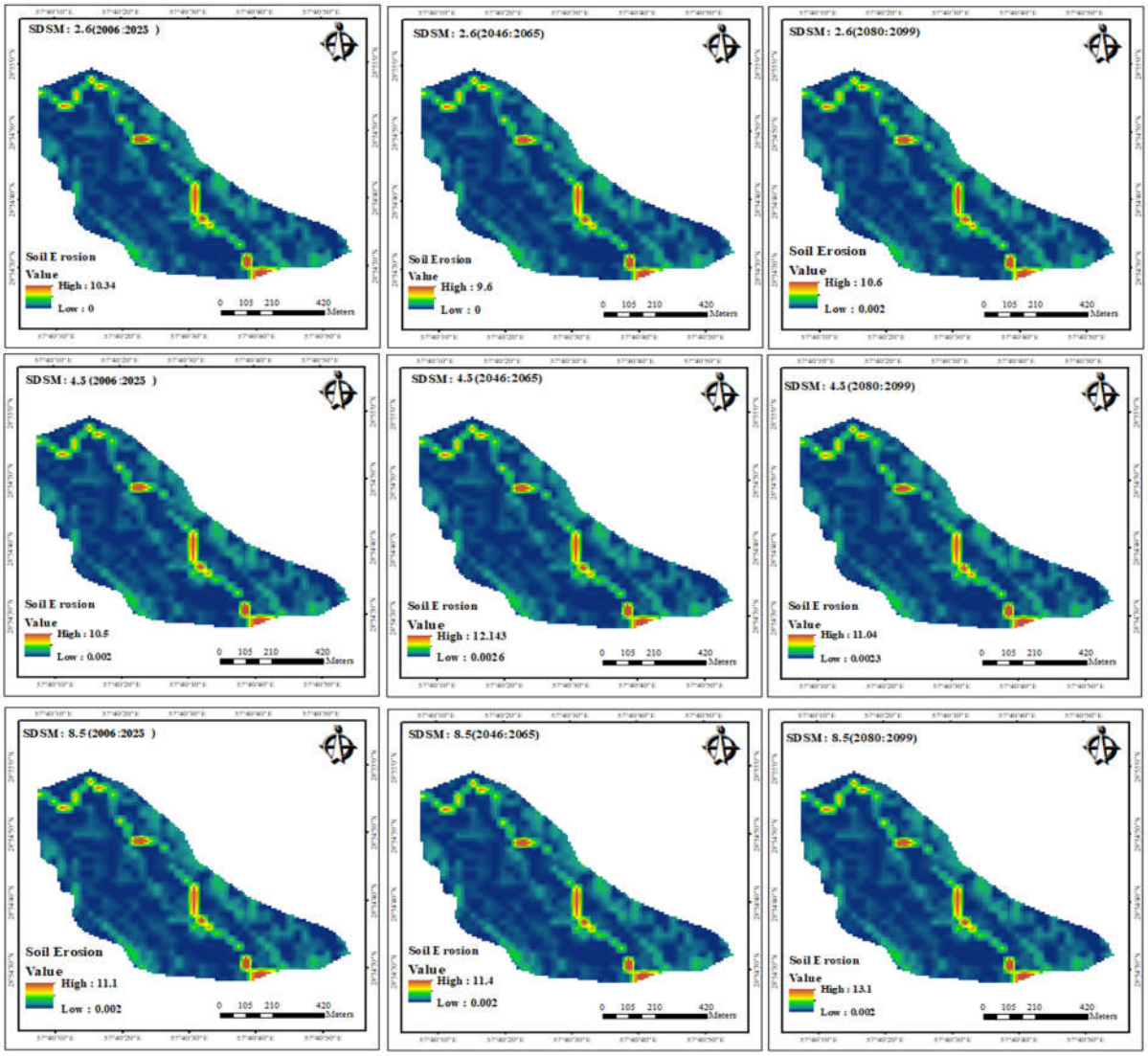

Figure (8): Variation of soil erosion risk under different scenarios for three periods in Anar Sheitan region

The effect of climate change on the estimation of soil erosion in Anar Sheitan forest and Tal Siah regions suggested that the overall trend of soil water erosion was relatively constant at different periods due to the small size of the study area, but despite the limited surface area, the effect of these changes on erosion risk is evident. According to the results, of the soil erosion risk would peak in both regions under RCP8.5 scenario during 2080-2099 period. The soil erosion will continue to rise in the future if the current situation persists.

Since soil erosion leads to soil loss and sediment transport to low lands and running water, it can have a negative impact on open and closed water ponds. Therefore, reducing soil erosion and preventing sediment transport can prevent adverse effects, which lead to the soil infertility, and surface and ground water pollution, thus preventing the economic and environmental loss (Mohammadi et al, 2018). Therefore, the implementation of watershed management activities in the regions, including methods of Tecomella Undulata proliferation, construction of artificial forests and seeding can increase aggregates by improving the ground cover, and ultimately reducing the soil loss.

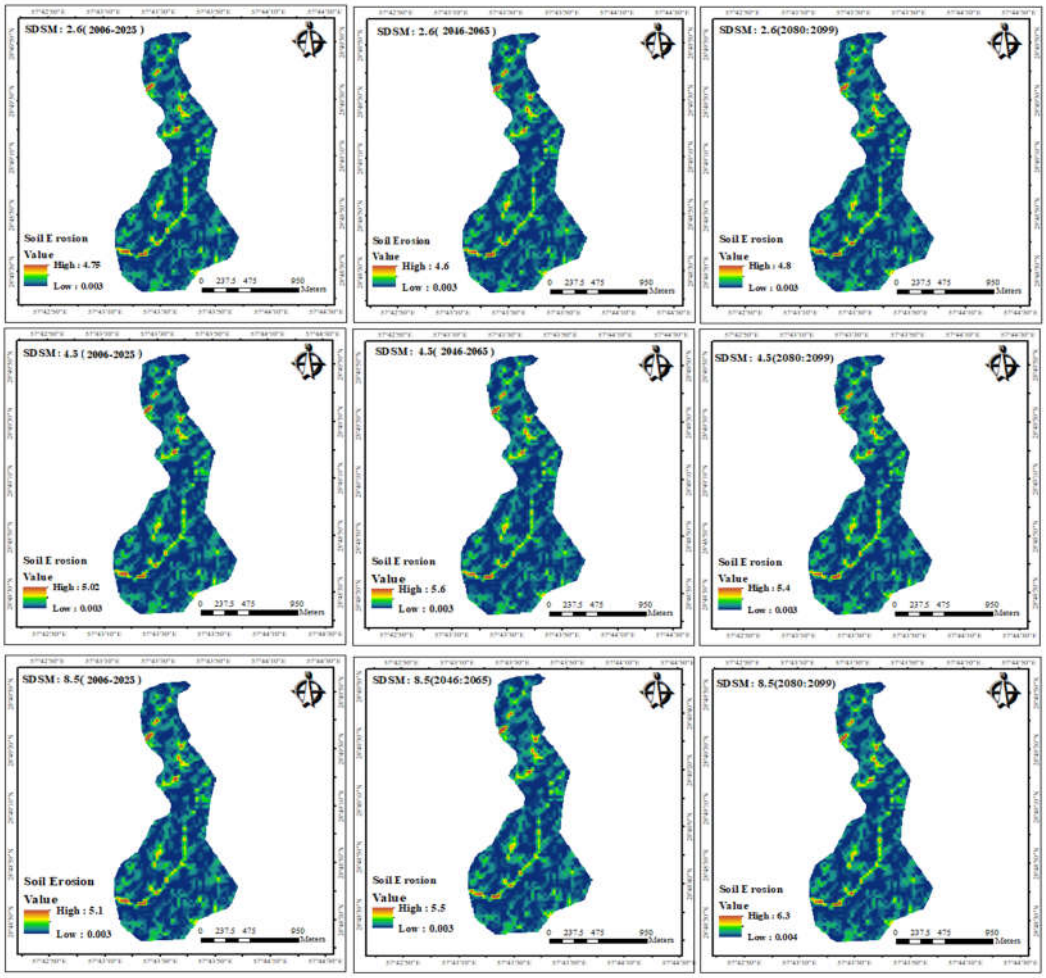

Figure (9): Variations of soil erosion risk in different scenarios for three periods in Tal Siah region

4. Conclusion

Creating databases by traditional methods (like cartography) is very time-consuming, tedious, and impractical. However, the GIS and RS can be effectively used to develop managerial strategies and provide selective options for managers to solve the soil erosion problem. The effects of climate change on soil erosion have attracted the attention of many researchers in the world in recent years. Therefore, the present study aimed to investigate the effects of climate change on risk of soil erosion in protected forest (Anar Sheitan) and artificial forest (Tal Siah) using remote sensing and GIS techniques in different scenarios. Results of the study indicated that maximum and minimum average soil erosion values belonged to 2080-2099 and 2006-2025 respectively. Soil erosion difference in various regions is more dependent on the regional topography; and the changes in amounts of soil erosion in different scenarios indicated the impact of climate change on rainfall erosivity factor in different periods. In general, results of the present study indicated that considering future scenarios, the amount of soil erosion would increase compared to the current situation; hence, the soil management and conservation will be essential to prevent economic, social and environmental damage in the regions. In other words, the use of proper managerial measures (especially soil and vegetation) can control or decrease the soil erosion in the regions as much as possible. The present study provides valuable information for managers and policy makers in sustainable development planning of the regions to make decisions by a better understanding of the

regions. The method can be also utilized for different regions of Iran.

Acknowledgments

This research is part of a research project financed by the University of Jiroft no: 4812_97_2.

Refrences

1. Amiri, I., Sodaiezade, H., Mosleh Arani, A., Taie Semiromi, J., Hakimzade, M.A, 2019. Autecology of Tecomella undulata (Roxb.) Seem in southern Iran. Journal of Forest and Poplar Research, 26 (4):506-519. (in Persian with English abstract)
2. Anache, J.A., Bacchi, C.G. and Alves-Sobrinho, T, 2014. Modeling of (R) USLE C-factor for pasture as a function of Normalized Difference Vegetation Index. European International Journal of Science and Technology, 3(9), 214-221.
3. Asadi, H., Honarmand, M., Vazifedoust, M., & Mousavi, A, 2017. Assessment of Changes in Soil Erosion Risk Using RUSLE in Navrood Watershed, Iran. Journal of Agricultural Science and Technology, 19(1): 231-244.
4. Asadi, H., Jafari, M., Asharfzadeh, A., Sharifi, A, 2018. Forecasting the effect of climate change on soil erosion hazard in Navrood watershed. Iranian Journal of Water and Soil Conservation. 2018; 25(2): 235-250.
5. Azimi Sardari, M.R., Bazrafshan, O., Panagopoulos, T., Rafiei Sardooi, E, 2019. Modeling the Impact of climate change and land use change scenarios on soil erosion at the Minab Dam Watershed. Sustainability, 11(12): 3353. DOI: 10.3390/su11123353
6. Bedoui, Ch, 2019. Predicting water erosion in arid lands using the GIS-based RUSLE model: A case study of Bedour catchment, central Tunisia. Journal of water and Land Development. Vol 40 (1-3): 59-66. DOI: 10.2478/jwld-2019-0006.
7. Fathizad, H., Karimi, H., Alibakhshi, S.M, 2014. The estimation of erosion and sediment by using the RUSLE model and RS and GIS techniques (Case study: Arid and semi-arid regions of Doviraj, Ilam province, Iran). International Journal of Agriculture and Crop Sciences, 7(6): 304-314.
8. Ferreira, V., Panagopoulos, T., Andrade, R., Guerrero, C., Loures, L, 2015. Spatial variability of soil properties and soil erodibility in the Alqueva reservoir watershed. Solid Earth, 6(2): 383-392.
9. Gaubi, I., Chaabani, A., Mammou, A.B. and Hamza, M.H, 2017. A GIS-based soil erosion prediction using the revised universal soil loss equation (RUSLE) (Lebna watershed, Cap Bon, Tunisia). Natural Hazards, 86(1):219-239.
10. Gee G.W. and Bauder J.W. 1982. Particle-size analyses In: Klute, A. (Ed.), Method of Soil Analyses, Part 1: Physical and Mineralogical Methods, 2nd ed. American Society of Agronomy, Madison, WI, 383–411.
11. Hassan, Z., Shamsudin, S. and Harun, S, 2014. Application of SDSM and LARS-WG for simulating and downscaling of rainfall and temperature. Theoretical and applied climatology, 116(1-2):243-257.
12. Hengl, T., 2006. Finding the right pixel size. Computers & geosciences, *32*(9):1283-1298.
13. Honarmand, M., Asadi, H., Vazifedoost M., Moussavi A. Evaluation of soil erosion risk using RUSLE, GIS and RS in Navrood watershed. Proceeding of the 12th Iranian Soil Science Congress, 3-5 September 2011, University of Tabriz, Tabriz, Iran.
14. Hoomehr, S., Schwartz, J.S., Yoder, D.C, 2016. Potential changes in rainfall erosivity under GCM climate change scenarios for the southern Appalachian region, USA. Catena, 136:141-151. DOI: 10.1061/41173(414)148
15. Kardavani, P. Conservation Soil, 8th ed. Tehran: Tehran University Press, 2005. (In Persian).
16. Lin, C.Y., Lin, W.T. and Chou, W.C, 2002. Soil erosion prediction and sediment yield estimation: the Taiwan experience. Soil and Tillage Research, 68(2:143-152. DOI: 10.1016/S0167-1987(02)00114-9

17. Lu, D., Li, G., Valladares, G.S., Batistella, M, 2004. Mapping soil erosion risk in Rondonia, Barzilian Amazonia using RUSLE, remote sensing and GIS. Land Degradation and Development, 15: 499-512.
18. Mohammadi, Sh., Karimzadeh, H.R., Alizadeh, M. 2018. Spatial estimation of soil erosion in Iran using RUSLE model. Iran Journal of Eco Hydorolgy, 5(2): 551-569.
19. Moore, I.D., Burch, G.J, 1986. Physical basis of the length-slope factor in the universal soil loss equation 1. Soil Science Society of America Journal, 50(5):1294-1298.
20. Moore, I.D., Wilson, J.P, 1992. Length-slope factors for the Revised Universal Soil Loss Equation: Simplified method of estimation. Journal of soil and water conservation, 47(5):423-428.
21. Nearing, M.A., Pruski, F.F. and O'neal, M.R, 2004. Expected climate change impacts on soil erosion rates: a review. Journal of Soil and Water Conservation, 59(1):43-50.
22. Nikkammi, D., Mahdian, M.H, 2015. Rainfall erosivity mapping in Iran. Journal of Watershed Engineering and Management. 6(4): 364-376. (in Persian)
23. Nord, G.; Esteves, M. PSEM_2D: A physically based model of erosion processes at the plot scale. Water Resour. Res. 2005, 41, W08407
24. Panagopoulos, T., Cakula, A., Ferreira, V., Arvela, A, 2015. Simulation model for predicting soil erosion in a large reservoir of southern Portugal. International Journal of Sustainable Agricultural Management and Informatics, 1(1), p.3À25.
25. Panagos, P., Borrelli, P., Meusburger, K., Yu, B., Klik, A., Lim, K.J., Yang, J.E., Ni, J., Miao, C., Chattopadhyay, N., Sadeghi, S.H.R, 2017. Global rainfall erosivity assessment based on high-temporal resolution rainfall records. Scientific Reports, *7*(1), p.4175.
26. Patowary, S. and Sarma, A.K., 2018. GIS-based estimation of soil loss from hilly urban area incorporating hill cut factor into RUSLE. Water resources management, *32*(10):3535-3547.
27. Prasannakumar, V., Vijith, H., Abinod, S. and Geetha, N, 2012. Estimation of soil erosion risk within a small mountainous sub-watershed in Kerala, India, using Revised Universal Soil Loss Equation (RUSLE) and geo-information technology. Geoscience Frontiers, 3(2):209-215.
28. Renard K.G. 1997. Predicting soil erosion by water: a guide to conservation planning with the revised universal soil loss equation (RUSLE), 1997.
29. Renard, K.G., Freimund, J.R., 1994. Using monthly precipitation data to estimate the R-factor in the revised USLE. Journal of hydrology, 157(1-4):287-306.
30. Renard, K.G., Foster, G.R., Weesies, G.A. and Porter, J.P., 1991. RUSLE: Revised universal soil loss equation. Journal of soil and Water Conservation, 46(1):30-33.
31. Roodab Paydar Consulting Engineers, 2011. Detailed studies of forest resources management plan in Tal Siah area, ministry of Agriculture. (in Persian)
32. Sadeghi, S.H.R., Hazbavi, Z, 2015. Trend analysis of the rainfall erosivity index at different time scales in Iran. Natural Hazards, 77(1):383-404.
33. Schuol, J., Abbaspour, K.C., Srinivasan, R., Yang, H, 2008. Estimation of freshwater availability in the West African sub-continent using the SWAT hydrologic model. Journal of hydrology, 352(1-2):30-49.
34. Segura, C., Sun, G., McNulty, S., Zhang, Y, 2014. Potential impacts of climate change on soil erosion vulnerability across the conterminous United States. Journal of Soil and Water Conservation, 69(2):171-181.
35. Sharifi, A., Shirani, H., Besalatpour, A.A., Esfandiarpour Borujeni, I, 2020**.** Effect of forest and pasture land uses on interrill erosion and some of soil physical properties in southern Iran. Journal of Water and Soil, 34(2): 455-469.
36. Teng, H., Rossel, R.A.V., Shi, Z., Behrens, T., Chappell, A., Bui, E, 2016. Assimilating satellite imagery and visible–near infrared spectroscopy to model and map soil loss by water erosion in Australia. Environmental Modelling & Software, 77:156-167.
37. Van Vuuren, D.P., Edmonds, J., Kainuma MRiahi, K., Thomson, A., Hibbard, K., Hurtt, G.H., Kram, T., Krey, V., Lamarque, J.F.,

Masui, T., et al, 2011. The representative concentration pathways: An overview. Climatic. Chang. 109(1): 5–31.

38. Walkley, A., Black, I.A, 1934. An examination of digestion methods for determining soil organic matter and a proposed modification of the chromic and titration. Soil science society of America journal, 37: 29-38.
39. Wilby, R.L., Harris, I, 2006. A framework for assessing uncertainties in climate change impacts: Low□flow scenarios for the River Thames, UK. Water resources research, 42(2).
40. Wischmeier, W.H., Smith, D.D, 1978. Predicting rainfall erosion losses: a guide to conservation planning (No. 537). Department of Agriculture, Science and Education Administration.
41. Yang, X., Yu, B., Xie, X, 2015. Predicting changes of rainfall erosivity and hillslope erosion risk across greater Sydney region, Australia. International Journal of Geospatial and Environmental Research, 2(1), p.2.
42. Zare, M., Nazari Samani, A.A., Mohammady, M., Teimurian, T., Bazrafshan, J, 2016. Simulation of soil erosion under the influence of climate change scenarios. Environmental Earth Sciences, 75(21), p.1405. DOI:10.1007/s12665-016-6180-6